Surface & Coatings Technology 358 (2019) 726–731

Contents lists available at ScienceDirect

Surface & Coatings Technology

journal homepage: www.elsevier.com/locate/surfcoat

Electron beam nitriding of titanium in medium vacuum

V.A. Burdovitsin[a], D.A. Golosov[c], E.M. Oks[a,b], A.V. Tyunkov[a,b], Yu.G. Yushkov[a,b], D.B. Zolotukhin[a,*], S.M. Zavadsky[c]

[a] Tomsk State University of Control Systems and Radioelectronics, 40 Lenin Avenue, Tomsk 634050, Russia
[b] Institute of High Current Electronics SB RAS, 2/3 Academichesky Ave., Tomsk 634055, Russia
[c] Belarusian State University of Informatics and Radioelectronics, 6 P. Brovki Str., Minsk 220013, Belarus

ARTICLE INFO

Keywords:
Electron beam and plasma nitriding
Fore-vacuum plasma-cathode electron sources
Titanium
Nitride coatings

ABSTRACT

We describe a novel method for electron-beam nitriding of metal (titanium) under medium (fore-vacuum) pressures (2–8 Pa) of nitrogen. Titanium sample was heated by a dc electron beam generated by a fore-vacuum plasma-cathode electron source with current up to 100 mA and energy up to 8 kV; this beam also generated beam-produced plasma with active nitrogen atoms, ions and other reactive species near the sample. SEM chemical composition analysis of the nitride layer have shown the presence of approximately 25 wt% of N, wt. 68% of Ti and only wt. 6% of O atoms within the processed layer. The X-ray diffraction spectrum of the nitride sample showed that the modified layer has a crystalline structure predominantly orientated along the crystallographic directions (111), (200), (220), characteristic of δ-TiN with a face-centered lattice. Besides the δ-TiN phase, there are present in the nitrided layer a γ phase of Ti_2N (tetragonal nitride) with predominant orientation (200). These results show the advantage of using forevacuum sources for electron beam and plasma nitriding of metals.

1. Introduction

Nitriding of metals is a widely known technique for enhancing the operating properties of materials in engineering [1–3]. There are commonly used three types of nitriding: gas nitriding [1], salt bath nitriding [2], and plasma nitriding [3]. Among these types of nitriding processes, plasma nitriding has the advantage of being technologically short-timed, environmentally pollution-free, and low gas- and energy-consuming [4]. These features promote the wide use of plasma nitriding for improving hardness, corrosion and wear resistance of various types of steel [5,6] and titanium [7].

Direct current plasma nitriding (DCPN) has been industrially used for the last 40 years [6]. This method does not have the shortcomings of gas and liquid nitriding. Nevertheless, with a glow discharge, the processed sample is a part of the glow discharge cathode at high voltage (of the order of 600–700 V). This can damage the surface because of arc formation, as well as overheat sharp edges leading uneven nitriding of the surface layers [3,6]. A method of active screen plasma nitriding (ASPN) is being developed lately [3,4,6]. The nitriding workpiece is placed at floating potential inside a perforated hollow screening electrode made of the same material as the sample, which serves as cathode of the glow discharge generated between it and the vacuum chamber. This approach bypasses the disadvantages of the DCPN method while preserving (and in some regimes improving) the operating properties of the nitrided samples.

However, the ASPN nitriding method, as well as DCPN, is characterized by a long nitriding process time (4–12 h), with a typical nitrided layer thickness of 10 μm. Also, in ASPN, the dimensions of nitriding samples are limited by the size of the grid. In addition, since heating of the nitriding sample occurs due to thermal radiation of the mesh screen, most of the input power is consumed inefficiently. An additional disadvantage of the ASPN method is sputtering of the screen, which limits its lifetime and leads to sometimes undesirable deposition (in case of mismatching) of its material on the sample to be nitrided.

Another alternative method, basically free of these drawbacks, is electron beam plasma nitriding (EBPN) [8–12]. The authors of [8] used the electron beam as a beam plasma generator. The processed samples were placed in direct vicinity of the electron beam at negative voltage (−350 V). The samples were heated up by an external source and the vacuum chamber was filled with an argon-nitrogen mixture at a pressure of 21.3 Pa. Using the electron beam plasma, they achieved an increase of the micro-hardness of AISI 316 steel by several factors. In Refs. [9–12], the electron beam was used to both generate plasma and heat the sample. The authors kept the sample temperature at the required level through variation of the beam parameters. The pressure of the argon-nitrogen mixture was 0.1–1 Pa and the accelerating voltage was

* Corresponding author.
E-mail address: ZolotukhinDen@gmail.com (D.B. Zolotukhin).

https://doi.org/10.1016/j.surfcoat.2018.11.081
Received 9 October 2018; Received in revised form 24 November 2018; Accepted 26 November 2018
Available online 30 November 2018

hundreds of volts. The authors succeeded to achieve improved hardness of the sample surface layers, which, as in Refs. [6, 8, 11], was attributed primarily to the presence of atomic nitrogen near the processed workpiece because the nitriding process was carried out with the electron beam energy close to the nitrogen molecule dissociation maximum by electron impact (60–140 eV). Despite indirect confirmation of this conjecture (color change and increased hardness of the sample), no mass-to-charge or optical measurements of the beam plasma ions were conducted.

Forevacuum electron sources with plasma cathodes [13], operating in the medium vacuum range of pressure 1–100 Pa [14], enable successful processing and sputtering not only of conductive materials [15,16] but dielectrics as well [17,18]. Such possibility arises from the fact that negative charge accumulated on the surface of the dielectric is compensated by the plasma ions generated when the electron beam propagates through the inert or active gas medium. The use of forevacuum sources for nitriding has an important advantage: the possibility to independently vary the current, beam energy, and gas pressure enables one to establish the required temperature regime for the nitriding workpiece without using any additional bias power supply or heating. The range of working pressure and parameters of the electron beam (current and voltage) applied during irradiation of metallic samples (for example, titanium and various kinds of stainless steel) can significantly affect the nitriding layer parameters. One should expect here that increased forevacuum gas pressure (several to tens of pascals) will be lead to intensification of the nitriding process in the electron beam plasma.

The purpose of this work was to investigate the possibility of nitriding titanium in the electron beam plasma generated by a forevacuum electron source under direct irradiation of the titanium sample by the electron beam; and to characterize the modified surface layer by studying the mass-to-charge composition of the beam plasma ions, tribological properties, micro-hardness, X-ray and elemental analysis of the nitrided surface.

2. Experimental setup

2.1. Electron source

The electrode system of the plasma electron source used in the experiments is shown in Fig. 1.

The electron beam gun consists of an electron optical column (Fig. 1), which includes cathode, anode, extractor, focusing and cooling systems. The upper section of the column contains hollow anode *1*, with a water-cooling jacket, and further down a cooled anode *2*. The cathode and anode are made of stainless steel. The anode-cathode discharge gap is bridged by a standard high voltage insulator *5*. To stabilize the plasma boundary and prevent it from "dumping out" to the accelerating gap, we used a 1 mm thick perforated plate 3 (emission electrode) made of tantalum. The anode is attached to the extractor flange through the high voltage insulator of the accelerating gap (the space between the emission electrode and the extractor). Extractor *4* (the accelerating electrode) is detachable, made of stainless steel and has a conical shape. The extractor is cooled by the running water to provide optimal temperature when operating in continuous mode. An electromagnetic focusing system 7 is used to focus the electron beam. The focusing coil is made of copper wire wound around a stainless steel frame. The main operating parameters of the source are given in Table 1.

Table 1
Electron source operating parameters.

Operating mode	Continuous
Discharge current	Up to 1 A
Accelerating voltage	Up to 20 kV
Beam current	Up to 300 mA
Beam diameter at a distance not exceeding 30 cm from the focusing system	5–10 mm
Maximal achievable electron beam power	6 kW
Working gas	Residual atmosphere, helium, air, oxygen, nitrogen, argon, and others
Working gas pressure	1–30 Pa – optimal 100 Pa - maximal

2.2. Experimental parameters

The experimental setup used for nitriding of titanium is shown in Fig. 2. The plasma source *1* was mounted on the vacuum chamber flange *8*. The plasma electron source was fed by constant voltage sources connected to the discharge and accelerating gaps. On applying a discharge voltage between anode and cathode, a glow discharge started to burn. Electrons were extracted through a perforated plate. In the anode-extractor gap, upon applying accelerating voltage U_{acc}, the electrons were accelerated and initial formation of the beam occurred. The formed electron beam entered the magnetic field of the short-focus magnetic coil where its formation was finalized. Along its way to the processed sample, the electron beam ionizes the gas in the working

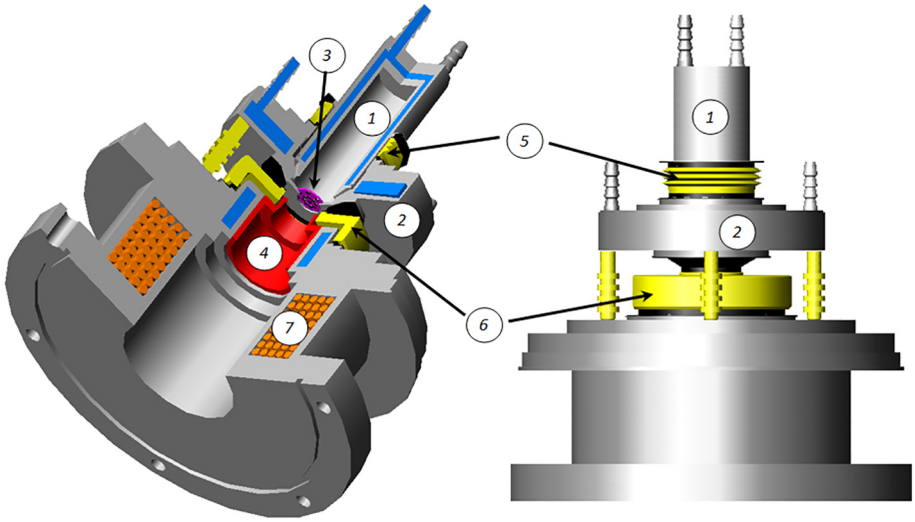

Fig. 1. Electrode system of the electron source: 1 – cylindrical hollow cathode; 2 – anode; 3 – perforated plate (emission electrode); 4 – extractor; 5, 6 – ceramic high voltage insulators; 7 – electromagnetic focusing system.

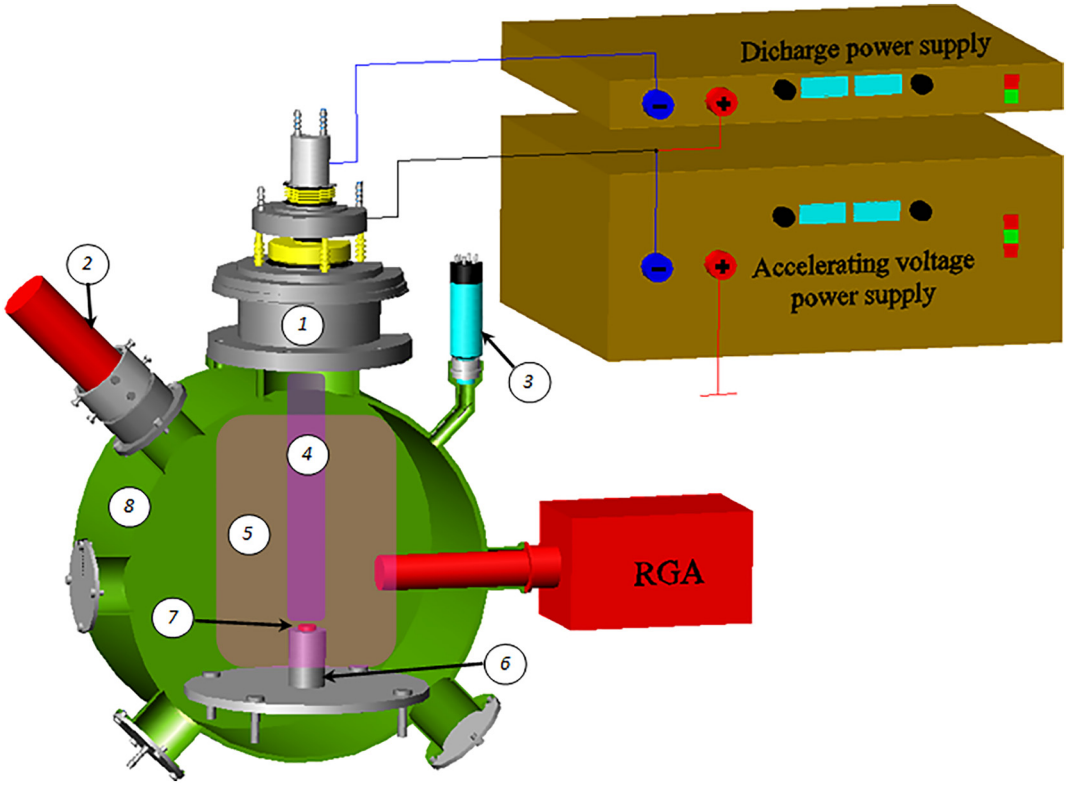

Fig. 2. Experimental setup: 1 – electron source; 2 – infrared pyrometer; 3 – vacuum sensor; 4 – electron beam; 5 – beam plasma; 6 – tantalum crucible; 7 – titanium sample; 8 – section view of the chamber walls.

chamber and produces the beam plasma. The electron beam interacting with the sample surface heats it up.

The working chamber was first pumped out to a pressure of $5 \cdot 10^{-3}$ Pa, using a turbomolecular pump nEXT300D with a speed of 300 l/s, followed by nitrogen injection to a pressure of 8 Pa. During the nitriding process, the beam current and the accelerating voltage were respectively 100 mA and 6 kV, and the process duration was 75 min. The sample temperature was monitored by a remote Raytek optical pyrometer and was 900 °C.

Since increased hardness of the surfaces of the worked pieces is considered to be related to the presence of atomic nitrogen, we carried out mass-to-charge analysis of the constituents of the beam plasma ions in order to determine optimal parameters of the electron beam for nitriding. Investigation of the mass-to-charge composition of the beam plasma ions was conducted using a modified mass-to-charge quadrupole analyzer of residual atmosphere RGA-100 with aperture located in the direct vicinity of the nitriding sample. The measurement details and analyzer design are discussed in [19]. Since the nitriding process suggests long and intense heating of the sample, and hence, of the nearby region, the analyzer was removed during the process to prevent damage to the mass-separator sealing and insulators.

2.3. Sample

For the sample we used sheet titanium BT1-0, 4 mm thick, of which an element of size 10 × 10 mm was cut out. The side of the sample subject to electron beam irradiation was polished by abrasive paper, and before being installed in the vacuum chamber, wiped with ethanol. The sample was mounted on a tantalum crucible and was electrically grounded.

2.4. Equipment and techniques used to study the modified layer

The surface and cross-section microstructure, nitride layer thickness as well as the sample chemical composition, were studied using a Hitachi S3400N scanning electron microscope equipped with a Bruker X'Flash 5010 energy-dispersion microanalyzer.

X-ray phase analysis (XPA) of the modified layer was performed using a Shimadzu XRD-6000 diffractometer with monochromatized Cu Kα radiation in gliding beam geometry. Phase analysis was done using the database PDF 4+ and software for full profile analysis POWDER CELL 2.4. The XPA is based on X-ray diffraction on the crystal lattice of the studied material. Applying the XPA method to the sample under study, we determined the phase composition, dimensions of the coherent scattering regions (CSR), lattice parameters and lattice deformation (Δd/d) of the formed layer.

Tribological characteristics at room temperature were measured using a tribometer. The tribometer used the ball-on-disk measurement technique. The tested sample is subject to a load of 2 N from a spherical tip. The tip is installed on a rigid lever, which is in fact a frictionless force sensor. The tip was made of tungsten carbide. The friction coefficient was determined during the tests by measuring the deflection of the elastic lever. The wear of material is determined by measuring the track left during the test. The wear parameter V, indicative of the rate of wearing, is determined by the formula $V = 2\pi RA / FL$, where R is the track radius, μm; A is the cross-section area of the wear slot, μm^2; F is the exerted load, N; L is the length of the ball's path, m.

A Leika VMHT Mot micro-hardness tester with Knoop indenter was used to measure Knoop hardness (*HK*). The indenter exerted a load of 5–50 g on the coating surface for a duration of 7 s.

3. Results and discussion

It is known that mainly nitrogen atoms play the leading role in ion-plasma nitriding of metal samples [20]. Therefore, using the modified RGA-100 designed to analyze mass-to-charge ratios of plasma ions, we were able to monitor the fraction of nitrogen atoms in the plasma assuming that the fraction of nitrogen atomic ions is directly proportional

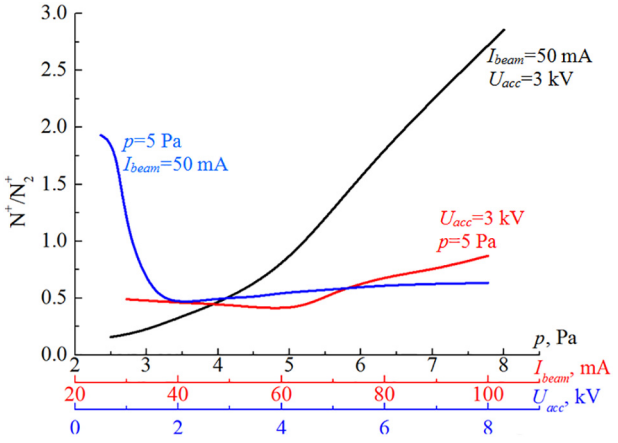

Fig. 3. Dependence of the ratio of atomic to molecular nitrogen ions on the experimental parameters.

Table 2
Some reactions producing atomic and molecular nitrogen ions and their cross sections.

	Reaction	Cross-section (10^{-20} m^2) at the electron energy			Ref.
		100 eV	500 eV	2000 eV	
1	$e + N_2 = N_2^+ + 2e$	2.615	1.428	0.521	[21]
2	$e + N_2 = N + N + e$	1.9	0.3	0.09	[22]
3	$e + N = N^+ + 2e$	1.58	0.826	0.3	[23]
4	$e + N_2 = N^+ + N^{2+} + 3e$	0.7	0.3	0.02	[24]

to the fraction of neutral nitrogen atoms. Fig. 3 shows the signal intensity ratio of nitrogen atomic to molecular ions depending on the experimental parameters (pressure, beam current, and the accelerating voltage). Fig. 3 demonstrates that with increasing pressure the fraction of atomic nitrogen ions in the beam plasma grows practically linearly. An increase of the beam current in the interval from 30 to 100 mA also leads to an increase of the concentration of atomic nitrogen ions by almost two times. With increase of accelerating voltage in the range 500–1000 V, there is observed a sharp decrease of the number of atomic nitrogen ions. Further increase of the accelerating voltage, and hence of the beam energy, practically has no effect on the fraction of atomic or molecular nitrogen ions. The observed trends can be explained by examining the cross-sections of the most active reactions in the plasma that result in the production of atomic and molecular nitrogen ions by the accelerated electron beam (Table 2).

It follows from Table 2 that the reaction cross-sections leading to generation of molecular ions (Reaction 1) dominate, both for low and high beam energies. However, at small beam energies (near the maximum of the ionization cross-section for 100 eV and below), the role of dissociation (Reaction 2) dramatically increases and results in increased generation of atomic nitrogen and its ionization (Reaction 3). This fact can explain the high ratio of N^+/N_2^+ at low energies observed in Fig. 3. With increasing beam energy, the cross-section for dissociation of molecular nitrogen by electron impact drops sharply [22]. This explains the decline in the ratio of N^+/N_2^+ with increasing beam energy up to 2000 eV. Increase of the N^+/N_2^+ ratio with increasing gas pressure is most likely connected with increased intensity of inelastic scattering of electrons on molecules at higher gas pressure. This results in a lower average energy of the electron beam, which, again, leads to increased dissociation and the growth of the fraction of atomic ions. Thus, it follows from Fig. 3 and Table 2 that the most effective way of generating atomic nitrogen by the electron beam in forevacuum is a mode with low beam energy (500–1000 eV) at a high gas pressure (7–10 Pa). However, in order to ensure sufficient temperature for the nitriding process in the present experiment, the accelerating voltage was increased to 6 kV; at this, the sample temperature reached 900 °C.

By recording the X-ray characteristic radiation with the help of the scanning electron microscope (SEM), we determined the chemical composition of the cut of the modified layer (Fig. 4).

The prevailing elements are titanium and nitrogen with the presence of oxygen and a small quantity of carbon, though the total concentration of the latter two does not exceeds 6.2 wt%. Small quantities of oxygen and carbon contained in the modified layer are due to their presence in the near-surface layer of titanium and, as shown in [25], such quantities do not degrade the nitrided layers. The modified layer thickness was 8 μm for a duration of the nitriding process of 75 min.

The X-ray structural analysis did not reveal any presence of carbide phases (Fig. 5). However, there were detected oxide phases corresponding to TiO_2 and Ti_2O_3 (Fig. 5 and Table 3). According to the small percentage of oxide phases, the oxide takes up an insignificant part of

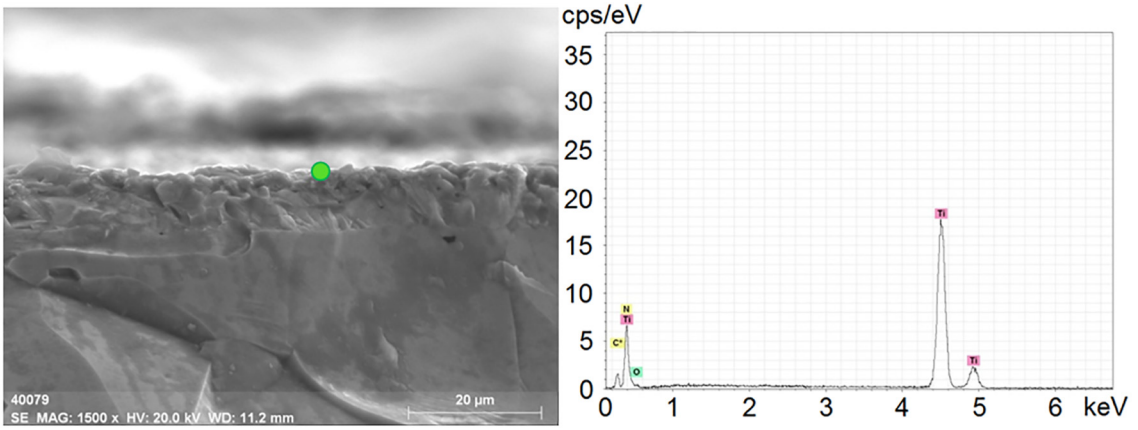

Element	AN	series	Net	[wt.%]	[norm. wt.%]	[norm. at.%]	Error in wt.% (1 Sigma)
Carbon	6	K-series	720	0	0	0	0
Nitrogen	7	K-series	2865	34,61255233	25,12569431	49,61779438	6,073055593
Oxygen	8	K-series	172	8,529543521	6,191704705	10,70438571	3,478288836
Titanium	22	K-series	26593	94,61549963	68,68260098	39,67781991	2,718530531
			Sum:	137,7575955	100	100	

Fig. 4. Results of SEM measurements.

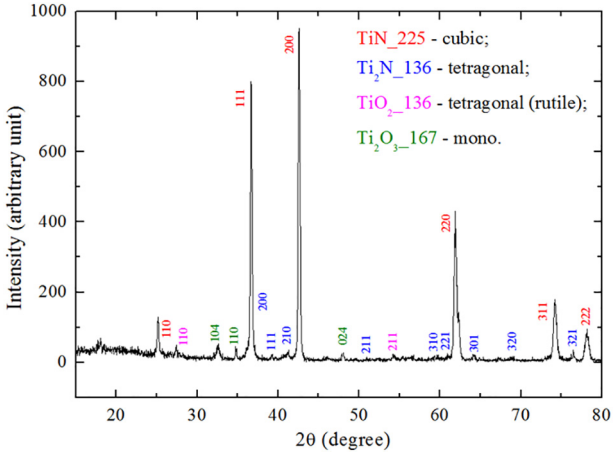

Fig. 5. X-ray diffraction spectrum.

Table 3
Results of the X-ray structural analysis.

Phases	Phase contents, mass %	Lattice parameters, Å	CSR size, nm	$\Delta d/d \times 10^{-3}$
TiN_225	72	a = 4.2328	89	1.3
Ti_2N_136	18	a = 4.8754 c = 3.1340	29	1.8
TiO_2_136	3	a = 4.5803 c = 2.9780	62	0.5
Ti_2O_3_167	7	a = 5.1656 c = 13.6954	17	2.3

the sample volume and comes from its presence on the original surface. The results of X-ray structural analysis completely corroborate the SEM data.

According to Fig. 5, the modified layer has a crystalline structure predominantly orientated along the crystallographic directions (111), (200), (220), characteristic of δ-TiN with a face-centered lattice. The intensity peaks (110), (311) и (222) are manifested weaker. Besides the δ-TiN phase, there are present in the nitrided layer a γ phase of Ti_2N (tetragonal nitride) with a predominant orientation (200). Other phases are weakly manifested. The reflections of the main peaks of δ-TiN (111), (200) are narrow and the size of the crystal grains are on a level of 89 nm, which testifies to large residual stress in the formed layer. In addition, as shown in [26], titanium nitride with the predominant orientation (200) has improved mechanical properties.

The results of tribological investigations (Figs. 6 and 7) showed that the modified layer of titanium nitride and the surface of the original sample had a friction coefficient whose average values were $\mu = 0.436$ (Fig. 6) for titanium and $\mu = 0.495$ (Fig. 7) for the modified layer. From the cross-sectional area of the wear track (Figs. 6 and 7), we calculated the wear parameter *V*, indicative of the rate of wearing, for the original titanium sample and for the modified layer of titanium nitride. Its magnitude for titanium ($1.6 \cdot 10^6$ μm^3/N·m) was several orders of magnitude larger than that for the titanium nitride layer ($4.1 \cdot 10^3$ μm^3/N·m).

The latter value is typical for conventionally-formed TiN layers (the wear parameter is greater than 3000 μm^3/N·m). These indices allow one to expect a longer service life of titanium parts nitrided by the electron beam in forevacuum. It is worthy to note that the hardness of the nitrided layer (2150 HK) has increased practically by ten times as compared with the hardness of the original Ti surface (225 HK).

4. Conclusion

We have demonstrated the possibility of nitriding of titanium in an electron beam plasma by direct electron beam irradiation from a forevacuum electron source. The energy-dispersion spectra of the nitrided layer testify to the prevailing presence of titanium and nitrogen with

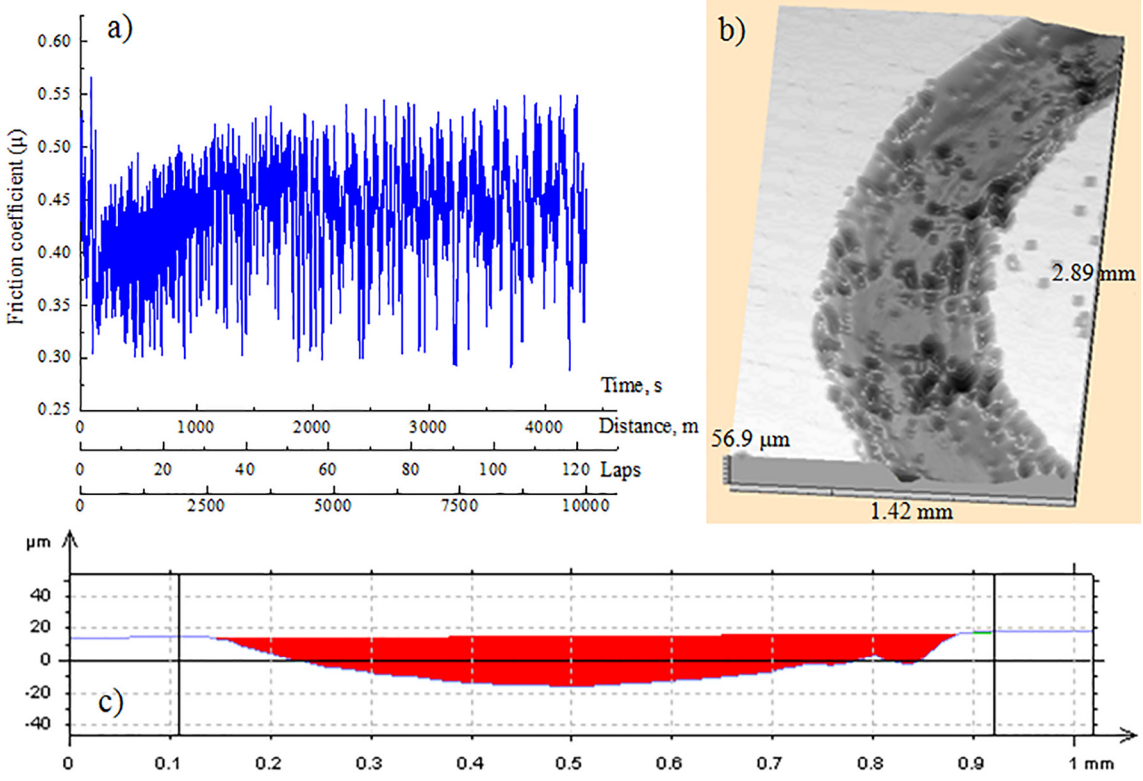

Fig. 6. Tribological investigation of the original titanium surface: a) friction coefficient as a function of testing parameters; b) photo of the wear track on the surface of the sample, c) cross-sectional profile of the wear track.

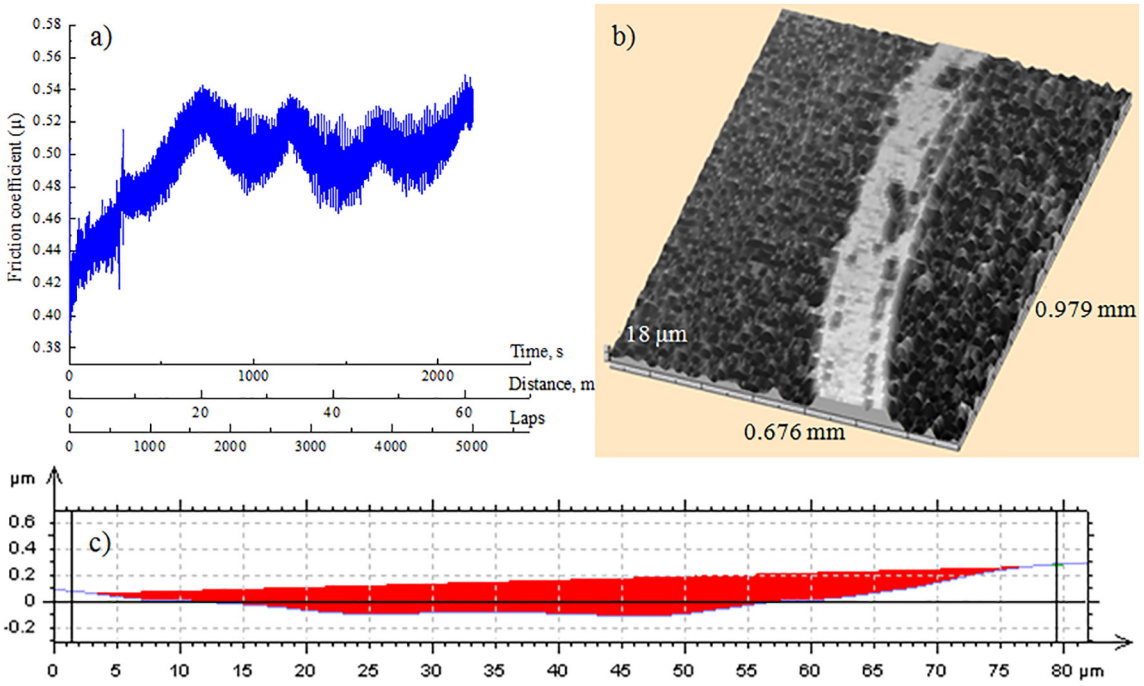

Fig. 7. Tribological investigation of the titanium nitride surface: a) friction coefficient as a function of testing parameters; b) photo of the wear track on the surface of the sample, c) cross-sectional profile of the wear track.

insignificant traces of carbon and oxygen. The X-ray structural analysis revealed the polycrystalline structure of the nitrided layer with predominant orientation along the crystallographic directions (111), (200), (220), characteristic of δ-TiN with a face-centered lattice. Hardness and tribological studies of the surface layers showed small values for the coefficient of friction and a multiple increase of wear and hardness of the nitrided surface as compared with the original titanium sample. The obtained results demonstrate the possibility of using the forevacuum sources for beam plasma nitriding of metals.

Acknowledgement

The work was supported by the joint Russian – Belarusian research program grant #18-58-00004 (Russian Foundation for Basic Research) and the grant #T18P-092 (Belarusian Republican Foundation for Fundamental Research).

References

[1] José Francisco dos Santos, Carlos Mario Garzón, André Paulo Tschiptschin, Improvement of the cavitation erosion resistance of an AISI 304L austenitic stainless steel by high temperature gas nitriding, Mater. Sci. Eng. A 382 (2004) 378–386.
[2] Jun Wang, Yuanhua Lin, Jing Yan, Dezhi Zen, Qiang Zhang, Runbo Huang, Hongyuan Fan, Influence of time on the microstructure of AISI 321 austenitic stainless steel in salt bath nitriding, Surf. Coat. Technol. 206 (15) (25 March 2012) 3399–3404.
[3] H. Nii, A. Nishimoto, Surface modification of ferritic stainless steel by active screen plasma nitriding, J. Phys. Conf. Ser. 379 (2012) 012052.
[4] Akio Nishimoto, Kimiaki Nagatsuka, Ryota Narita, Hiroaki Nii, Katsuya Akamatsu, Effect of the distance between screen and sample on active screen plasma nitriding properties, Surf. Coat. Technol. 205 (2010) S365–S368.
[5] L.N. Tang, M.F. Yan, Influence of plasma nitriding on the microstructure, wear, and corrosion properties of quenched 30CrMnSiA steel, J. Mater. Eng. Perform. 22 (7) (July 2013) 2121–2129.
[6] C. Zhao, C.X. Li, H. Dong, T. Bell, Study on the active screen plasma nitriding and its nitriding mechanism, Surf. Coat. Technol. 201 (6) (4 December 2006) 2320–2325.
[7] J. Sun, W.P. Tong, L. Zuo, Z.B. Wang, Low-temperature plasma nitriding of titanium layer on Ti/Al clad sheet, Mater. Des. 47 (May 2013) 408–415.
[8] C. Muratore, D. Leonhardt, S.G. Walton, D.D. Blackwell, R.F. Fernsler, R.A. Meger, Low-temperature nitriding of stainless steel in an electron beam generated plasma, Surf. Coat. Technol. 191 (2005) 255–262.
[9] P. Abraha, Y. Yoshikawa, Y. Katayama, Surface modification of steel surfaces by electron beam excited plasma processing, Vacuum 83 (2009) 497–500.
[10] N.V. Gavrilov, A.S. Mamaev, Low-temperature nitriding of titanium in low-energy electron beam excited plasma, Tech. Phys. Lett. 35 (8) (2009) 713–716.
[11] Ryuta Ichiki, Yuusuke Kubota, Masashi Yoshida, Yuji Fukuda, Yasuyuki Mizukamo, Tamio Hara, Surface nitriding of light metals using electron-beam-excited-plasma (EBEP) source, J. Plasma Fusion Res. SERIES 8 (2009) 1408–1411.
[12] N.V. Gavrilov, A.I. Men'shakov, Effect of the electron beam and ion flux parameters on the rate of plasma nitriding of an austenitic stainless steel, Tech. Phys. 57 (3) (March 2012) 399–404.
[13] V.A. Burdovitsin, E.M. Oks, Fore-vacuum plasma-cathode electron sources, Laser Part. Beams 26 (4) (December 2008) 619–635.
[14] A.A. Zenin, A.S. Klimov, V.A. Burdovitsin, E.M. Oks, Generating stationary electron beams by a forevacuum plasma source at pressures up to 100 Pa, Tech. Phys. Lett. 39 (5) (May 2013) 454–456.
[15] A.V. Tyunkov, Yu.G. Yushkov, D.B. Zolotukhin, K.P. Savkin, A.S. Klimov, Generation of metal ions in the beam plasma produced by a forevacuum-pressure electron beam source, Phys. Plasmas 21 (2014) 123115.
[16] D.B. Zolotukhin, E.M. Oks, A.V. Tyunkov, Y.G. Yushkov, Deposition of dielectric films on silicon using a forevacuum plasma electron source, Rev. Sci. Instrum. 87 (6) (1 June 2016) (P. 063302).
[17] Y.G. Yushkov, A.V. Tyunkov, E.M. Oks, D.B. Zolotukhin, Electron beam evaporation of boron at forevacuum pressures for plasma-assisted deposition of boron-containing coatings, J. Appl. Phys. 120 (23) (21 December 2016) (P. 233302).
[18] E.M. Oks, A.V. Tyunkov, Y.G. Yushkov, D.B. Zolotukhin, Ceramic coating deposition by electron beam evaporation, Surf. Coat. Technol. 325 (25 September 2017) 1–6.
[19] D.B. Zolotukhin, A.V. Tyunkov, Yu.G. Yushkov, E.M. Oks, Modified quadrupole mass analyzer RGA-100 for beam plasma research in forevacuum pressure range, Rev. Sci. Instrum. 86 (2015) (P. 123301).
[20] G.G. Tibbets, Role of nitrogen atoms in "ion-nitriding", J. Appl. Phys. 45 (11) (1974) 5072–5073, https://doi.org/10.1063/1.1663186.
[21] W. Hwang, Y.-K. Kim, M.E. Rudd, New model for electron-impact ionization cross sections of molecules, J. Chem. Phys. 104 (1996) 2956.
[22] S.G. Walton, D.R. Boris, S.C. Hernandez, E.H. Lock, Tz.B. Petrova, G.M. Petrov, R.F. Fernsler, Electron beam generated plasmas for ultra low Te processing, ECS J. Solid State Sci. Technol. 4 (6) (2015) N5033–N5040.
[23] Y.-K. Kim, J.-P. Desclaux, Ionization of carbon, nitrogen, and oxygen by electron impact, Phys. Rev. A 66 (012708) (2002).
[24] Yukikazu Itikawa, Cross sections for electron collisions with nitrogen molecules, J. Phys. Chem. Ref. Data 35 (2006) 31.
[25] A.D. Korotaev, V.Yu. Moshkov, S.V. Ovchinnikov, Yu.P. Pinzhin, A.N. Tyumentsev, V.P. Sergeev, D.P. Borisov, V.M. Savostikov, Multicomponent hard and superhard submicro- and nanocomposite coatings on the basis of titanium and iron nitrides, Phys. Mesomech. 10 (3–4) (2007) 156–167.
[26] J. Pelleg, L.Z. Zevin, S. Lungo, Reactive-sputter-deposited TiN films on glass substrates, Thin Solid Films 197 (1991) 117–128.